Information Fusion 53 (2020) 4–19

Contents lists available at ScienceDirect

Information Fusion

journal homepage: www.elsevier.com/locate/inffus

Environment-fusion multipath routing protocol for wireless sensor networks

Xiuwen Fu[a], Giancarlo Fortino[b,*], Pasquale Pace[b], Gianluca Aloi[b], Wenfeng Li[c]

[a] Shanghai Maritime University, Haigang 1550 avenue, Shanghai 201306, China
[b] University of Calabria, Italy
[c] Wuhan University of Technology, China

ARTICLE INFO

Keywords:
Wireless sensor networks
Environment-aware
Multipath routing
Potential field

ABSTRACT

In most cases, wireless sensor networks (WSNs) are deployed in unattended scenarios and are featured by energy sensitivity and low cost, thus making the performance of WSNs prone to the impact of external environment and internal energy. Existing routing protocols attempted to optimize the energy efficiency and routing reliability from the perspective of the network itself and failed to take into consideration the environmental impact from outside, causing them cannot make prompt reactions to the dynamic changes of the environments (*e.g.,* wildfire). Thus, in these routing protocols the routing survivability under harsh environments is questionable. To tackle this issue, the paper proposes an environment-fusion multipath routing protocol (EFMRP) to provide sustainable message forwarding service under harsh environments. In EFMRP, routing decisions are made according to a mixed potential field in terms of depth, residual energy and environment. The basic idea of this approach is to instruct data packets to select routes with the best trade-off among latency, energy conservation and routing survivability. As the environmental field is constructed and updated using the sensing capability of WSN itself, constructed routes can avoid crossing through the danger zones to keep the paths safe. To enhance the performance of EFMRP, specific maintenance, traffic allocation and retreat mechanisms are proposed. We investigate the impact of configuration parameters and paths number on the routing performance respectively and compare EFMRP with respect to commonly used routing protocols. The experimental results show that EFMRP can obtain significant improvements in packet delivery ratio and network lifetime under harsh environments.

1. Introduction

Wireless sensor networks (WSNs) are usually made up of hundreds even thousands of distributed sensor nodes organized in ad-hoc paradigm to monitor environments. Since they can be easily deployed and self-organized, WSNs can cover a wide range of application domains. As in most of the scenarios WSNs are expected to operate in unattended environments and powered by batteries, the network performance would be easily affected by the energy factor and the environmental factors; therefore, how to guarantee stable data delivery is always the most significant concern of WSNs [17,21]. Nowadays, multipath routing protocols have been considered as the most effective way to maintain high quality data transmission. In fact, using single path routing, if the delivery path is cut off due to node/link failure, the data transmission would be aborted; on the contrary, the interruption of a single path would not stop the data delivery from sensor nodes to the sink in case of multipath routing. Besides that, compared with the single path routing, the energy consumption would be more balanced in the network by implementing the multipath routing [1,9,37,38]. In view of the above advantages of multipath routing, numerous multipath routing protocols have been proposed in the literature. Most of them focus on the energy efficiency and routing reliability, namely finding the optimal multipath to maximize the reliability and minimize the energy consumption [10,11,19,33].

However, in our opinion, besides energy and reliability, environment-awareness is another factor that needs to be carefully considered in the design of multipath routing. Due to the large-scale deployment reason, the cost of a single sensor node is always very limited, making the nodes likely to be influenced by environmental factors (e.g., temperature, humidity, electromagnetic interference and vibration). For instance, high temperature would increase the malfunction probability of sensor nodes and excessively high temperature would burn the sensor nodes eventually. Excessively high humidity would raise the short-circuited probability of sensor nodes and decrease the link quality. Strong electromagnetic interference would cause a dramatic increase in the data loss rate. Therefore, aiming to lower

* Corresponding author.
E-mail address: fuxiuwen1987@163.com (X. Fu).

https://doi.org/10.1016/j.inffus.2019.06.001
Received 28 February 2019; Received in revised form 16 May 2019; Accepted 1 June 2019
Available online 3 June 2019

the impact of environmental factors on routing performance as much as possible, we should try to avoid the constructed multipath passing through the "danger zone" (*i.e.,* the zone under harsh environmental conditions). Considering, for example, the wildfire monitoring, besides fire detection, another responsibility of fire-alarming WSNs is to deliver real-time data of fire scene to the head-quarter to help make the rational fire-management strategy. If the routing protocol fails to perceive the environment changes and the data packets still follow the routes that would cross the fire zones, the data delivery would be cut off immediately once relay nodes are burned. But for environment-aware routing, once it senses the fire threats, it would adjust its delivery paths in real time to avoid passing through dangerous areas, and thus the data delivery would not cease.

Therefore, aiming to make the routing protocol more invulnerable to the environmental impact, we develop an environment-aware multipath routing protocol called EFMRP based on the use of three independent virtual *potential fields* such as environment, depth and residual energy. The environmental field is to ensure that the constructed multipath avoid danger area. The depth field is to make data packets reach the sink. The residual energy field is to make sensor nodes prone to select their neighbors with more residual energy as next-hop relays. The final routing is constructed to satisfy the three virtual potential fields at the same time. The major contributions of EFMRP are summarized as follows.

1. High routing reliability under the harsh environmental conditions: based on the environmental data acquired by sensor nodes, the environmental field is able to instruct data packets avoid crossing the danger zones. What is more, a maintenance mechanism is designed to ensure the network being proactive about environmental threats.
2. High energy efficiency and low delivery latency: energy field and depth field are involved in the routing to ensure messages selecting the routes with low delay and high energy efficiency. Moreover, a traffic allocation scheme is developed for load balance in order to further prolong the network lifetime.

The remainder of this paper is structured as follows: Section 2 describes the related work. In Section 3, we illustrate our basic idea and motivations behind EFMRP. Technical details on how to correctly design the *potential fields* in EFMRP are presented in Section 4. Maintenance mechanism, traffic allocation mechanism and retreat mechanism are presented in Section 5 to guarantee the routing operate efficiently. In Section 6, we investigate the impact of parameters on the routing performance of EFMRP and compare it with respect to commonly used routing protocols. Finally, the conclusions are drawn in Section 7.

2. Related work

The concept of multipath routing dates back to 1990s, of which the initial purpose was to enhance the error tolerance and load balance of mobile ad-hoc networks. Later on, multipath routing has been deemed as an effective tool to break through the bottlenecks of WSNs in reliability and energy efficiency [12–15]. The related work can be classified into two categories according to the node/path disjointness: node-disjoint and partially-disjoint.

Regarding the node-disjoint multipath, there is no common node or link among the discovered paths. The multipath built from the source node to the sink guarantees that any node or link failure can only interrupt the routing path it belongs and would not affect other paths. Therefore, the reliability of node-disjoint routing protocols is higher than partially-disjoint routing. To the best of our knowledge, N-to-1 routing protocol is the first node-disjoint routing protocol [29]. The basic idea of N-to-1 routing protocol consists in the implementation of a spanning tree in the network by using a simple flooding strategy. Each branch represents a node-disjointed path. Although the implementation of N-to-1 routing protocol is quite easy, it requires multiple rounds of message flooding in the routing discovery phase, resulting in energy overconsumption. H-SPREAD [30] is an improved version of N-to-1 routing protocol. By introducing the threshold secret sharing mechanism in H-SPREAD, even when a certain number of paths failed, messages can still be restored at the sink. However, since its multipath discovery process is still the same as N-to-1 routing protocol, the energy efficiency still remains the main bottleneck.

The authors in [27] proposed a delay-constrained high-throughput node-disjoint multipath protocol called DCHT. In this protocol, multipath can be built by a direct diffusion process. Data transmission latency and interference strength are the major criteria to judge the quality of constructed paths. However, since the interference strength is fast-changing WSNs, routing synchronization of DCHT would occupy lots of network resources.

In [43], an energy-efficient and collision-aware node-disjoint multipath protocol named EECA was presented. The network is divided into two sides based on the straight line between the source-destination pair and then the source node discovers an independent path in each side. The advantage of EECA is that the mutual interference of multipath could be lowered as they are in two separated zones, but the upper limit of the multipath number is 2.

In [25], a geographic node-disjoint multipath routing called GNPR is presented. In this routing, the sensor node discovers multipath greedily by selecting its direct neighbor with the smallest angle to the sink. By using this greedy-compass technique, sensor nodes can discover all node-disjoint paths. GNPR performs well in terms of end-to-end delay.

In WSNs, the so called "hot spot" issue consisting in a much faster energy-depleting speed of the sensor nodes near the sink than other nodes [22], is faced by the authors in [42] whose designed a pairwise directional geographical routing named PWDGR. In their mechanism, pairwise nodes are equally selected in 360° scope around the sink. The node-disjoint paths can be built following the route "source to a pairwise node to the sink". In this way, the traffic flow around the sink can be assigned evenly and the "hot spot" issue can be much relieved. It is worthy of note that, as the sensor nodes in GNPR, EECA and PWDGR need to be equipped with GPS modules to access location information, the cost of network hardware would be huge in the cases of large-scale deployment.

In [26], the authors abstracted the node-disjoint discovery problem as the constrained *Steiner-tree* problem and solved this problem based on a multi-objective genetic algorithm. Energy, reliability and transmission delay are the optimization objectives. Since the Steiner-tree problem is NP-hard, this method can only be effective in the scenarios with a small number of sensor nodes and the routing mechanism is centralized because the solving process can only run in the sink. Similarly, in [28,34], the authors developed various optimization algorithms to find the node-disjoint multipath. Although computational efficiency was improved, the drawbacks showed in [26] still exist.

Despite the fact that node-disjoint multipath routing protocols demonstrate distinct advantages in term of reliability, in reality it would be difficult to find enough amounts of paths between sensor nodes and the sink in the cases of sparse deployment. Besides, the discovery of node-disjoint multipath always requires a frequent exchange of neighboring or global information, which would result in larger routing overhead. Therefore, some researchers attempted to relax the disjointness requirement in order to reduce the routing overhead and enhance the flexibility of applications. Based on this idea, partially-disjoint multipath routing was developed. Unlike node-disjoint, partially-disjoint multipath routing could include several shared nodes or links. Under this configuration, any node failure would interrupt all the paths that include the failure node. To the best of our knowledge, SAR is the first partially-disjoint multipath routing protocol implemented [45]. According to its routing mechanism, routing decisions were made based on three factors: energy conservation, QoS parameters, and level of packet priority in the traffic flow. SAR used a table-driven multipath approach that satisfies the QoS parameters, energy consumption, and fault tolerance. However, since the efficiency of SAR is closely related to its updating frequency of

routing tables in the sensor nodes, the overhead for routing maintenance is overwhelming.

ReInForM [8] employed a probabilistic flooding scheme to create multiple paths from the source to the sink. Each node is supposed to have knowledge of local channel errors. Reliability can be achieved by introducing redundancy in the form of copies of each packet sent through multiple paths. Unfortunately, the routing maintenance cost is too high owing to the frequent exchange of neighboring routing information. The proposals in [2,40] can be both considered as an upgrade version of ReInForm; their main improvement consists in making the sensor node with more resource have a higher probability to be selected as relays in the multipath.

Aiming to minimize the damages that can be caused by single-link attacks, a secure multipath routing solution was developed in [36]. The proposed solution includes two algorithms (*i.e.,* bound-control algorithm and lex-control algorithm). The bound-control algorithm formulates the solution as a maximum flow problem and the lex-control algorithm is used to solve this problem. The link-attack tolerance of this solution was proven, but the performance with respect to other QoS indexes has not been investigated yet. To protect the network from malicious attacks, a random dispersive multipath routing protocol was designed in [6]. Since the generated multipath is distributed over the network in a dispersed way, the network performance can be guaranteed in terms of load balance and interference avoidance.

Despite to the described solutions, our proposed scheme EFMRP uses a field-driven fusion method to make the routing decisions. There have already been some field-fusion routing protocols in WSNs, most of them used the natural fields of physical phenomena. In [4], inspired by the magnetism in physics, the authors devised a simple data dissemination mechanism in which the data packets are considered as metallic nails, thus they are attracted by the sink just like a piece of magnet. In [46], the authors developed a routing protocol by abstracting WSNs as an electrostatic field and the message routing process is regarded as the motion of electric charges. In a similar way, thermal field and hydrodynamic field were used to support WSNs routing in [3,24,41].

In the literature, the *potential field* was also used for message routing in WSNs. In this field, the sink will impose gravity on messages and attract them to the sink. Although the fields imposed by the natural laws make the message routing process in a more intuitive way, they can only provide basic routing function (*i.e.,* instructing messages to reach the sink in a decentralized way) and the routing quality (*e.g.,* delivery latency and energy consumption) are still far from satisfactory. Moreover, to the best of our knowledge, the existing field-driven routing methods are designed for single routing path optimization, multipath routing has not been investigated yet.

Some multipath routing protocols were designed using the concept of “gradient” which is similar to “field”. In these protocols, the gradient can be seen as a cost field to provide the node direction to forward data from high cost to low cost. In [20], the authors proposed a state-free gradient routing protocol called SGF. In its transmission stage, the data forwarder is selected among multiple candidate nodes through a distributed contention process. The probability that a candidate node wins the contention depends on the node’s gradient, channel condition and remaining energy. In [35], for the purpose of energy balance, routing protocol EBRP is proposed, whose gradient is constructed according to the depth, remaining energy and energy density. In general, the goals of existing gradient-based routing protocols are still limited to minimize the energy consumption.

From all the previous discussions, we can easily argue that, although many researchers have focused their works on the multipath routing issues, they only attempted to improve the routing performance from the network perspective without taking into consideration the possible impact of the external environment on the routing. However, in reality, due to the large-deployment and low-cost implementation, environmental factors could easily affect WSNs routing, making them cannot be ignored anymore. Potential field as a field-establish method, origin from the observation of gravity interaction, provides a new idea to implement multipath strategies also taking into account the environmental impact. Therefore, this paper proposes an environment-fusion multipath routing protocol for WSNs based on potential field, which can lower the negative effects of external environments on message delivery as well as maintaining high energy efficiency and relatively low end-to-end delay. To the best of our knowledge, the work presented in this paper fills a void in the area of environment-fusion multipath routing.

3. Motivations

In the last few years, most of the literature focuses on the routing performance improvement of WSNs attempting to find new solutions from the network perspective poorly considering the impact of the environments. However, since in most cases the duty of WSNs is to monitor the environments, the performance of such WSNs is closely related to the environments. In particular, the impact of the environments on WSNs is twofold:

1. *Performance degradation in external environments* – due to large-scale deployment and lost-cost implementation, the performance of WSNs can be easily affected by environments. The harsh environmental conditions (*e.g.,* high temperature, high vibration and strong electromagnetic interference), would degrade the routing performance of the network. Especially in some extreme cases (*e.g.,* forest fire), the network might suffer serious damages. Nevertheless, existing routing protocols cannot make prompt reactions to the environmental changes. Therefore, how to ensure the network is able to provide sustainable message delivery service under the harsh environmental condition, is a meaningful issue.
2. *Environment-awareness* – with the decreasing cost of sensors, it is very common to find wireless sensor nodes equipped with multiple sensing modules (*i.e.,* temperature, humidity and acceleration), providing sensor nodes more powerful ability to perceive the surrounding environments. How to fully use the obtained environmental data to improve the network performance by making more reasonable routing decisions, is also worth exploring.

In this challenging research context, the main motivation behind our proposal is to use environmental data, throughout an information fusion process, to lower the negative impact of the environment on message routing as much as possible.

Potential field method was initially proposed by O. Khatib in 1986 [23] and it is mainly used for path planning of mobile robots in an unknown environment. Its basic idea is to abstract the motion of robots in the unknown environment as the motion propelled by attractive force in a virtual potential field. In this field, the target position and obstacles would create attraction and repulsion to robots respectively. The attraction and repulsion would create the corresponding field according to specific field functions. The robots would bypass the obstacles and reach the destination by following the field descent direction created by the resultant force of attraction and repulsion. Since the potential field can be easily modeled and implemented with a satisfying guidance accuracy, it has been extensively applied.

In WSNs, sensor nodes collect environmental data and transmit to the sink via multi-hop. From the spatial distribution point of view, the data flow demonstrates an evident centripetal feature. The process of data flow converging in the sink is quite similar to the process of multiple robots reaching the destination. Therefore, it inspires us to consider the data packets that are needed to relay as the mobile robots, the sink as the robots destinations and the sensor nodes as the road signs that the robots need to follow in the moving process. In this context, the entire process of message routing in WSNs can be abstracted as the moving process of robots reaching the destination by following the road signs. Therefore, we can borrow the potential field method to tackle the routing issue in WSNs.

In our method, the sink will create attraction that will become weaker with the increasing number of hops toward the sink. As the road sign, the sensor node creates repulsion which is determined by its environmental sensing data and residual energy value. The repulsion is proportional to the harsh level of environments detected by sensor nodes and inversely proportional to the residual energy of the sensor nodes. Since the environmental data and the residual energy value change over time, the repulsion also changes dynamically. Therefore, by considering the resultant force of attraction and repulsion, on the one hand, EFMRP could be proactive to the changes of environments and adjust the routes promptly; on the other hand, when some nodes are threatened or destroyed by environmental factors, EFMRP could bypass the danger zone and discover safer paths to the sink.

4. Design of potential fields

In this section, we describe how to characterize the potential fields based on the fusion of different parameters such as depth, residual energy and environmental information of sensor nodes in order to generate a comprehensive potential field structure for message guidance by compounding environmental, depth and residual energy fields.

4.1. Environmental potential field

Since WSNs are always deployed in unattended environments, making sensor nodes vulnerable to the environmental factors during data transmission process, it would be reasonable to avoid the messages crossing through the danger zones in order to lower the environmental impact on the routing performance as much as possible, In fact, this routing-avoidance idea has been widely used in the robot navigation where robots are required to move away from the high-risk zones (*i.e.,* the areas with obstacles). Regarding the sensor nodes, on the one hand they can obtain the environmental data in their location easily by their own sensors; on the other hand, they can get the environmental data about their adjacent areas through the message exchange among neighboring nodes. In this manner, all the information prepared for field construction can be readily obtained. Aiming to make the proposed EFMRP environment-aware, here we design the following four environmental field functions.

4.1.1. Single environmental field

To quantify the impact of the environment on message routing, here we first define the single environmental field $U_s^k(i)$

$$U_s^k(i) = \begin{cases} \dfrac{D^k(i) - D^k_{\min}}{D^k_L - D^k_{\min}}, & D^k(i) < D^k_L, \\ 1, & D^k_L \le D^k(i) \le D^k_H, \\ \dfrac{D^k_{\max} - D^k(i)}{D^k_{\max} - D^k_H}, & D^k(i) > D^k_H, \end{cases} \tag{1}$$

where $U_s^k(i)$ is the environmental field created by sensor node i for the environmental factor k. $[D^k_L, D^k_H]$ is the normal operation interval of sensor nodes for the environmental factor k. If the environmental data $D^k(i)$ collected by node i is within the range $[D^k_L, D^k_H]$, we can consider that the performance of node i would not be affected by environmental factor k and then the single environmental field $U_s^k(i)$ is set to 1. On the contrary, $U_s^k(i)$ would be decreasing and the negative impact of environmental factor k on node i tends to be more evident. Aiming to normalize the single environmental field $U_s^k(i)$, we introduce $D^k_{\min}$ and $D^k_{\max}$ as the boundaries of environmental factor k, which means that the sampling data $D^k(i)$ for factor k are only allowed to float within the range $[D^k_{\min}, D^k_{\max}]$. Fig. 1 shows the trend of the function (1) representing the single environment field.

To further discuss on the reasonableness of the chosen trend for the curve in (1), we consider the most common environmental factor-temperature as an example. Obviously, if the sensor nodes are located in the high-temperature or low-temperature environments, their performance would suffer degradation and the malfunction probability would also be increasing sharply. By contrast, if the node is in the normal temperature environment, the impact of external temperature on node performance can be neglected. Here, assume that the normal operation interval of a sensor node is [0,50]°C, which means that the node could operate normally within this temperature interval and does not need to take into consideration the temperature factor. Only considering the general case, we set the temperature boundary as [− 10,100]°C, which means that the highest temperature and the lowest temperature of the deployment area is 100 °C and −10°C respectively. If the temperature sensed by the node i is 15 °C, the corresponding single environmental field created by the node i would be set equal to 1; but, if the sampling temperature rises to 80 °C, the generated $U_s^k(i)$ decreases to 0.4 which means that the routing cost of data packets passing node i is rising. Therefore, through the Eq. (1), we can properly guide data packets to choose the nodes under the more suitable environment as next hop, also avoiding to cross the dangerous area.

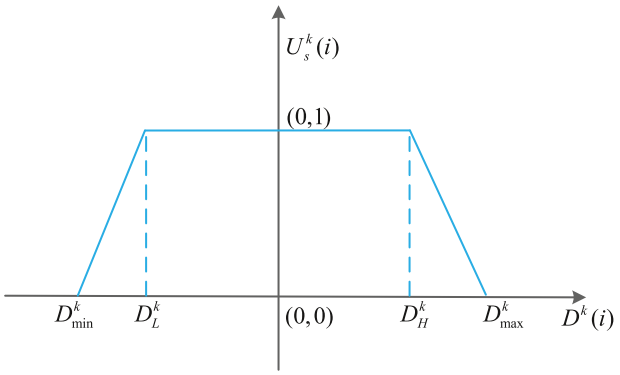

Fig. 1. Function curve of the Single Environment Field.

4.1.2. Multiple environmental field

Since the routing performance of WSNs is prone to be affected by multiple environmental factors, we design multiple environmental field $U_m(i)$ to quantify the impact of multiple environmental factors on the routing according to the following relation:

$$U_m(i) = \min\{U_s^k(i), \ldots, U_s^j(i)\}, \tag{2}$$

where $U_s^k(i)$ and $U_s^j(i)$ are the single environmental fields created by node i with respect to the environmental factors k and j. From the observation of reality, we can easily discover that there is a "barrel effect" in the routing process. In fact, if one of the multiple environmental factors would result in a too expensive routing cost, then the related node should not be selected as the relay node. Here we still use temperature as an example. Assume that the normal operation interval of a sensor node is [0,50]°C and the temperature boundary as [− 10,100]°C. If the temperature in one area is 100 °C, according to (1), we can get the temperature field generated by the nodes in this area is 0. For sensor nodes, this area can be definitely deemed as a "forbidden zone" because they can hardly survive in this area. Even though other environmental factors (*e.g.,* humidity and electromagnetic interference) have little negative effect on routing performance, the nodes in this area still should not be selected as next hop. Therefore, in the design of $U_m(i)$, we do not use average weighted method and choose the minimum field value among various environmental factors to represent multiple environmental field.

4.1.3. Neighboring environmental field

When a neighboring node detects an event (*e.g.,* wildfire) that would affect routing performance seriously, even though this event has not spread to the node itself, it also should be regarded as a potential threat. Therefore, aiming to keep constructed routes away from environmental

threats as early as possible, it is necessary to connect its own environmental field with the environmental field of its neighbors. Due to this reason, EFMRP defines the neighboring environmental field as follows:

$$U_n(i,j) = k_{ij} U_m(j), \tag{3}$$

where $U_n(i, j)$ is neighboring potential field of node i generated by its adjacent node j and k_{ij} is the attenuation coefficient, which can be calculated through the following equation

$$k_{ij} = 1 + \frac{L(i,j)}{R}. \tag{4}$$

where $L(i, j)$ is the distance between nodes i and j, R is the transmission radius of the sensor nodes and $U_m(j)$ indicates the environmental impact from the location area of node j on message routing.

The lower the $U_m(j)$ is, the stronger the environmental impact on routing tends to be. Thus, as the neighbor of node j, the potential threats that node i might face would also rise with the lowering of $U_m(j)$. Besides that, the threat level is also closely related to $L(i, j)$. It is easy to understand that the nearer distance $L(i, j)$ means that node i would be more prone to suffer the environmental threats from the location area of node j, reasonably explaining why $U_n(i, j)$ is designed to be proportional to $L(i, j)$ in (3) and (4). In particular, when $L(i, j)$=0, the positions of node i and j are overlapping. At this point, $U_n(i, j)$=$U_m(j)$, which means that the environmental impact on node j has been imposed on node i without loss. Since a sensor node always has multiple neighbors and each neighbor would generate an independent neighboring environmental field, we choose the minimum value of these fields as the final neighboring environmental field.

$$U_n(i) = \min\{U_n(i,j) | j \in \Omega(i)\}. \tag{5}$$

$U_n(i)$ is the neighboring environmental field of node i and $\Omega(i)$ is the collection consisting of neighbors of node i.

4.1.4. Environmental field

Finally, the environmental field of the generic sensor node i, is jointly determined by the multiple environmental field $U_m(i)$ and the neighboring environmental field $U_n(i)$. Without loss of generality, we can assume that neighboring environmental field $U_n(i, j)$ created by node j is the minimum among neighbors of node i. Through the normalization process, EFMRP can define the environmental field $U_e(i)$ of node i as

$$U_e(i) = \frac{U_m(i) + U_n(i)}{1 + k_{ij}}. \tag{6}$$

4.2. Depth potential field

To provide the basic routing function, namely to instruct packets to move towards the sink, we define the inverse proportional function of depth as the depth potential field $U_d(i)$.

$$U_d(i) = \frac{1}{d(i) + 1}, \tag{7}$$

where $d(i)$ denotes the depth of node i. The depth of a node is the number of hops along the shortest path from the sink. Then, the depth potential difference $V_d(i, j)$ from node i to node j is given by

$$V_d(i,j) = U_d(i) - U_d(j) = \frac{d(j) - d(i)}{(d(i)+1)(d(j)+1)}. \tag{8}$$

Since the depth potential function $U_d(i)$ is monotonically decreasing along with the depth of node i and the potential field value of the sink is 1 which is the highest in the network, the packets will reach the sink eventually by following the field-ascent direction and the fundamental routing function can be achieved. Regarding adjacent nodes i and j with depth n and $n + 1$ respectively, we can easily get the potential difference from node i to j

$$V_d(i,j) = \frac{1}{(n+1)(n+2)}. \tag{9}$$

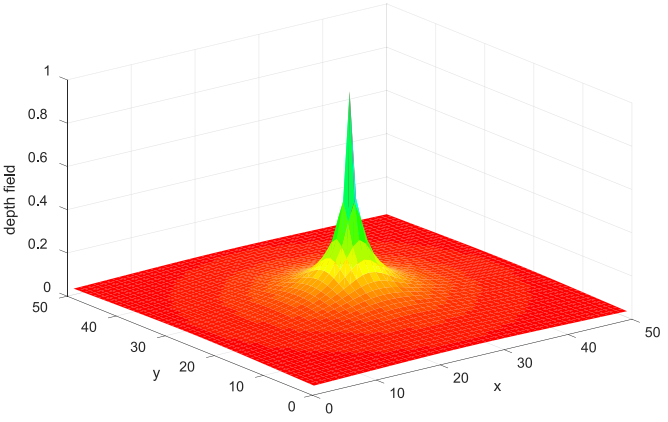

Fig. 2. Depth potential field.

Obviously, $V_d(i, j)$ is a fast decreasing function with the rise of n, which implies that the closer the packets approach to the sink, the stronger is the tendency that it moves towards the sink. For example, both the potential difference from depth $n = 2$ to 1 and from depth $n = 1$ to the sink (depth $n = 0$) are rather large: $V_d = 1/(1 + 1) - 1/(2 + 1) = 1/6$, $V_d = 1/(0 + 1) - 1/(1 + 1) = 1/2$. However, in the area far away from the sink (*i.e.,* large n), the centrality is quite weak. For instance, the depth potential difference from depth $n = 10$ to 9 is quite small: $V_d = 1/(1 + 9) - 1/(10 + 1) = 1/110$. In these "remote" areas, the impact of the depth potential field could not be dominant any longer and the possible disturbances caused by the other two fields could be more evident. In summary, this design characteristic could benefit the message routing in two aspects: 1) the potential field could drive the packets to reach the sink and this driving force tends to be stronger with the decreasing of depth; 2) the packets could choose appropriate routes (not only the shortest path) towards the sink as the message routing is prone to be affected by other two potential fields (*i.e.,* environmental field and energy field) in the area far away from the sink. Fig. 2 depicts the shape of a general depth potential field.

4.3. Energy potential field

Whit the aim of protecting the nodes presenting low energy levels, the proposed EFMRP scheme defines the energy potential field $U_g(i)$ using the residual energy of sensor nodes as follows

$$U_g(i) = E(i,t)/E_0, \tag{10}$$

where $E(i, t)$ is the residual energy of node i at time t. E_0 is the initial energy value. Without loss of generality, we reasonably assume that each node uses the same type of batteries which are fully charged in the initialization phase. Therefore, each sensor node has the same E_0.

4.4. Target potential field

The target potential field is a hybrid potential field created by mixing environmental field, depth field and energy field with the aim of instructing data packets to select routes having the best tradeoff among latency, energy conservation and routing survivability. Through the weighted sum method, we define target potential field $U_t(i)$ as

$$U_t(i) = (1 - \alpha - \beta)U_d(i) + \alpha U_e(i) + \beta U_g(i), \tag{11}$$

where $0 \le \alpha \le 1$, $0 \le \beta \le 1$ and $0 \le \alpha + \beta \le 1$. The weights α and β determine the impact of the environmental field and residual energy field on the routing decision. Obviously, when $\alpha = \beta = 0$, $U_t(i)$=$U_d(i)$, making messages follow the shortest paths to the sink. With the increasing of α, the impact of the external environment tends to be more significant and the packets are more inclined to choose the paths with higher invulnerability (*i.e.,* the routes with less environmental interference). Similarly,

with the rising of β, energy factor would play a more important role in message delivery and the packets tend to select the routes with more energy. This design would provide EFMRP with very high flexibility, as the users could customize the routing by adjusting parameters according to the task scenarios. When the network is in a relatively harsh environment, the user should set a relatively high α value. When the users turn their focus to extending the network lifetime, β should be set to a higher value. It is worthy to note that the target potential field of the sink is set to 1, the highest peak in the global field map, to ensure the messages arriving at the sink eventually.

4.5. Property of EFMRP

This section discusses the effects of parameters on the EFMRP scheme.

Proposition 1. *For node i in depth n, let $H = \{x | D(x) = n + 1, x \in \Omega(i)\}$. If $\alpha + \beta < \frac{2}{n^2+2n+2}$, $\forall h \in H$ will never be chosen as the next hop of node i.*

Proof. Let $L = \{x | D(x) = n - 1, x \in \Omega(i)\}$. Since environmental field and energy field are time-varying, $\forall h \in H$ and $\forall l \in L$, we can reasonable assume that the environmental field and energy field of node l and h at time t are $U_e(l, t)$, $U_e(h, t)$, $U_g(l, t)$ and $U_g(h, t)$ respectively. Then, we can easily get

$$U_t(l,t) = (1-\alpha-\beta)\frac{1}{n} + \alpha U_e(l,t) + \beta U_g(l,t). \tag{12}$$

$$U_t(h,t) = (1-\alpha-\beta)\frac{1}{n+2} + \alpha U_e(h,t) + \beta U_g(h,t). \tag{13}$$

Subtracting $U_t(h, t)$ from $U_t(l, t)$, we can obtain

$$\begin{aligned} U_t(l,t) - U_t(h,t) = (1-\alpha-\beta)\frac{2}{n(n+2)} + \alpha(U_e(l,t) \\ - U_e(h,t)) + \beta(U_g(l,t) - U_g(h,t)). \end{aligned} \tag{14}$$

For $U_e(l,t) - U_e(h,t)$, since $U_e(l, t)$ and $U_e(h, t)$ are greater than or equal to zero, when $U_e(l,t) = 0$ and $U_e(h,t) = 1$, the minimum value is -1. Similarly, we can get the minimum value of $U_g(l,t) - U_g(h,t)$ that is also equal to -1. Then, we can get

$$U_t(l,t) - U_t(h,t) > (1-\alpha-\beta)\frac{2}{n(n+2)} - (\alpha+\beta). \tag{15}$$

It is easy to understand that if $(1-\alpha-\beta)\frac{2}{n(n+2)} - (\alpha+\beta) \geq 0 \Rightarrow U_t(l,t) - U_t(h,t) > 0$. According to our routing mechanism, node i will choose node l rather than node h as next hop. $(1-\alpha-\beta)\frac{2}{n(n+2)} - (\alpha+\beta) \geq 0$ is equivalent to $\alpha + \beta \leq \frac{2}{n^2+2n+2}$. The proposition is proved. □

Remark 1. Proposition 1 describes the condition under which data packets will never be sent backward. We can see that when n is relatively large, $\alpha + \beta$ is quite small, i.e., the weight of the depth potential field would be quite large to avoid data packets being sent back to the nodes with higher depth. When n becomes smaller, $\alpha + \beta$ could be larger, but can still ensure data packets not being sent backward. Considering $n = 3$, $\alpha + \beta < 0.117$ can ensure no packets will be sent backward at the nodes with the depth value lower than 3; on the contrary, regarding the nodes with higher depth, some backward transmissions are allowed to balance the energy and avoid crossing through the danger zones.

The above proposition indicates the condition under which the shortest path will be chosen; however, different from the shortest path with only hop count as the metric, this shortest path also takes into consideration the environment and energy.

5. Design of multipath routing

To help sensor nodes make routing decisions, the input of EFMRP is the field values of sensor nodes which can be obtained through environmental sensing, message exchange with neighbors and their own state information. Since EFMRP follows a distributed routing paradigm, its output result is not to provide a complete path for each message at the source node, but to provide the IDs of the next-hop nodes for the message to guide it to the sink through multi-hop relays. The details on the design and implementation of EFMRP are described as below.

5.1. Field information

In this subsection, we discuss how EFMRP obtains the field information.

5.1.1. Depth

In the initialization phase, we design a limited flooding algorithm to help each node in the network to get depth information. Each sensor node would prepare a storage space for depth and the depth is initialized as *NULL*, except for the sink whose depth value is 0. The sink broadcasts a *HELLO* message to the network which includes the depth information of the last hop. Each sensor node will get its own depth by adding 1 to the depth value in the *HELLO* message and continue to transmit the *HELLO* message to its neighbors. If the sensor node has already updated its own depth value, it will compare its depth value with the depth value extracted from the *HELLO* message when receives the message again. Hereafter, according to the comparison result, it would decide whether update its own depth and continue to broadcast the *HELLO* message. It is worth noting that, to avoid excessive flooding over the network, *HELLO* message will contain a time stamp to record its generation time. Once the *TTL* (Time to Live) expires, the broadcasting process will be terminated.

5.1.2. Energy

EFMRP needs to know the residual energy on the local nodes, but the most popular WSN hardware platforms, such as MicaZ [39]and TelosB [7], are unable to directly provide such information. Luckily, we can add some extra hardware components, such as an A/D converter to estimate the residual energy by measuring the voltage value of the batteries. Besides that, a software solution is also feasible by estimating the consumed energy tacking into account the actions that the local node has performed. In this work, we assume that the value of the residual energy can be easily obtained from one of the above methods. This value will be sent within the updating message, thus every node knows the residual energy of all its neighbors and records them in the routing table.

5.1.3. Environment

To make the message routing aware of the environment, EFMRP needs to know the surrounding environmental information. In most cases, sensor nodes are equipped with multiple sensors. Among these sensors, temperature, acceleration and humidity are most common due to the task requirement and low-cost reason. Besides that, we can also add some extra sensors to support routing decision, such as electromagnetic sensors. In this work, we reasonably assume that the sensor nodes are well-equipped to get enough environmental information. By message exchange among neighbors, every node can obtain the surrounding environmental information to be stored in the routing table.

5.2. Path discovery phase

The application objects of EFMRP are the WSNs that are largely deployed in the harsh environment. On the one hand, these networks have strong demand for high reliability; on the other hand, their large-deployment feature provides enough flexibility for multipath design. Therefore, in EFMRP we choose the node-disjoint way to build multipath due to its highest reliability. The path discovery procedure is composed by the following three phases:

- **Initialization phase**: each sensor node maintains two tables in its own storage space: *FIELD_TABLE* and *ROUTING_TABLE*. The first one

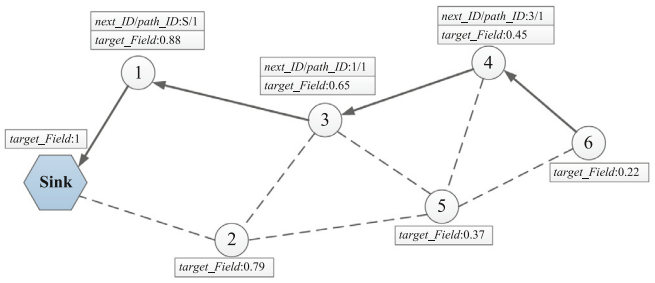

Fig. 3. Aa example of the primary path discovery.

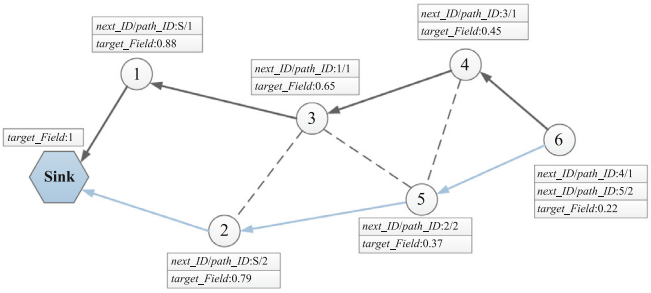

Fig. 4. An example of the secondary path discovery.

is used to store potential field values and the second is used to store the routing information. At first, the sink broadcasts a message to make the nodes aware of the depth. Then, each node broadcasts a message containing *node_ID, residual energy* and *environmental* values to its neighboring nodes. Upon receiving this message from neighboring nodes, each sensor node can have a clear picture of the state of its neighbors. After that, each sensor node can compute all the potential field values according to the acquired depth and neighboring information, and store them into *FIELD_TABLE*. Since the environment, energy and depth are time-varying, aiming to make the routing proactive to their changes, we design a maintenance mechanism to update potential field. The details can be found in Section 5.3.

- **Primary path discovery phase**: after the initialization phase, each sensor node can have all the target field information of its neighbors. When the source node creates a data packet, besides the specific sensed data, the data packet also includes *source_ID, path_ID, last_ID* and *destination_ID*. *source_ID* and *destination_ID* are the IDs of the source node and destination node respectively. In this work, the sink is the only destination and the *destination_ID* is set to 1. *last_ID* is the ID of the last hop and *path_ID* denotes the priority of paths whose allocation strategy will be described in Section 5.4. For the primary path, *path_ID* is set to 1. The source node chooses the node with highest target field value from its neighbors as the next hop. Finally, *next_ID* (the ID of next hop), *source_ID, path_ID* and *destination_ID* will be recorded as a row in the *ROUTING_TABLE*. When data packet reaches the next hop, the same operation continues until it reaches the sink. It is worth noting that, in order to avoid the data packet go back to the last hop, *last_ID* will be excluded when choosing next hop.
  Considering the simple topology shown in Fig. 3 as an example, we can assume that, through the initialization phase, each sensor node in the topology has already obtained the target field information. When the node 6 generates a data packet or need to relay a data packet from other sensor nodes, its *ROUTING_TABLE* is *NULL*. Through checking *FIELD_TABLE*, it would choose node 4 as the next hop because the node 4 have the highest target field value among its neighbors. Then, node 6 would add *source_ID*=6, *path_ID*=1, *next_ID*=4, *last_ID*=6 as a row in its *ROUTING_TABLE*. In the same way, when the data packet reaches node 4, it would choose node 3 as the next hop and update its *ROUTING_TABLE*. The process will continue until the complete construction of the primary path $6 \rightarrow 4 \rightarrow 3 \rightarrow 1 \rightarrow$ sink. When a new data packet is created in node 6 and is also assigned to be delivered by the primary path, through querying *source_ID* and *path_ID*, we can get *next_ID* in the same row, then next hop can be confirmed directly.
- **Secondary path discovery phase**: aiming to ensure the secondary path not overlapping with the primary one, in the discovery of the secondary path, the next hop would be the node with highest target field value except the node used by the primary path and its last hop. If the data packet is determined to follow the secondary path, *path_ID* would be labeled as 2. When the source node, generates a data packet that is assigned to the secondary path, it would send it to the node with second highest target field value. If the relay node receives the data packet labeled by the secondary path, it would broadcast a *QUERY* message to its neighbors to check whether they are used by primary path. According to the response results from its neighbors, it would choose the one with highest target field value among non-used nodes as the next hop. Other steps in the secondary path discovery are as same as those in the primary path discovery. It can be easily observed that, the only difference is that in the secondary path discovery the relay nodes are required to send a message to its neighbors to query non-used nodes. It is worth noting that this query process would only occur in the path discovery phase. Once the secondary path is constructed, the routing information would be stored in *ROUTING_TABLE*. When a new data packet labelled by the secondary path from the same source node arrives, the next-hop node can be easily determined through querying *next_ID* in *ROUTING_TABLE*.
  Looking the topology shown in Fig. 4 as an example, the primary path has already been built for the source node 6, which is $6 \rightarrow 4 \rightarrow 3 \rightarrow 1 \rightarrow$ sink; then, the secondary path is enabled for traffic balance. For the source node, through checking *path_ID*=1 in *ROUTING_TABLE*, we can get *next_ID*=4, which means node 4 has been used. Therefore, node 5 would be the next hop as it has the second highest target field. Upon receiving the data packet, node 5 queries its neighbors and node 2 would be selected as its next hop. Finally, we can get the secondary path $6 \rightarrow 5 \rightarrow 2 \rightarrow$ sink.

5.3. Routing maintenance

Since the residual energy of sensors nodes and the surrounding environment are time-varying, aiming to keep the built multipath proactive to these changes, it is necessary to design an effective routing maintenance mechanism. In EFMRP, two methods (*i.e.,* global maintenance and local maintenance) have been designed.

5.3.1. Local maintenance

When the sensor nodes do not have enough energy to support continued operation or their surrounding environment experience dramatic changes, they would inform their neighbors in order to make them proactive to these situations in the message routing.

For each sensor node i, when its residual energy $E(i) < \lambda_e$, the local maintenance mechanism will be triggered and then it will broadcast an alarming message *ALARM_EXHAUST* to its neighbors. After receiving the alarming message, the neighbors will set the target potential field of node i to 0 in their routing tables. Through this communication scheme, if the residual energy of a node is below the pre-configured threshold, it will not be selected as the relay node and its survival time will be prolonged significantly as its transmission task would only be constrained to deliver its own messages to the sink via multi-hop.

For sensor node i and environmental factor m, if node i meets (16), the local maintenance mechanism will be triggered.

$$|D_s^m(i,t) - D_s^m(i,t-1)| > \gamma(D_H^m - D_L^m), \tag{16}$$

where γ $(0<\gamma<1)$ is the environmental threshold. In this way, when the difference of measured values between $t-1$ and t with respect to the environmental factor m is larger than γ times of the size of $[D_L^m, D_H^m]$, the environment around node i is experiencing a dramatic change. At this point, node i will update its environmental field and target field according to the latest environmental data and broadcast the updated field values to its neighbors. These neighbors will update their routing tables and adjust their routing decisions accordingly.

5.3.2. Global maintenance

In practice, sensor nodes might fall into a sudden breakdown and some new nodes can join the network as the supplement, these joining or exiting behaviors of sensor nodes would result in the changes of the network depth information. Therefore, we need to introduce global maintenance into EFMRP to update the depth information over the network.

Unlike local maintenance that only occurs between adjacent nodes, global maintenance is started by the sink. The sink would flood an updating message *DEPTH_UPDATE* over the entire network periodically by introducing a timer T_{update}. When the initialization phase of the network is finished, the timer T_{update} is triggered. When $T_{update} = f_{update}$, the message *DEPTH_UPDATE* will be broadcasted to the entire network, then the network depth information would update and the timer T_{update} will be reset. f_{update} represent the updating frequency. If f_{update} is too large, the interval between two routing updating process would be too long, which would reduce the responsiveness of the routing towards the changes of the network topology. If f_{update} is too small, the message flooding process would occur too frequently, causing excessive overhead.

5.4. Traffic allocation

Once multiple paths have been discovered, the source node begins to transmit data packets to the sink. Since multiple paths are available, how to efficiently send these packets needs to be investigated. The main objective of traffic allocation is to decide the priority of multiple paths. In the most of the related work, the optimal principle has been widely used. In particular, the primary path is assigned for data forwarding and other paths would be alternative when the primary path is cut off. Although optimal principle would make better use of primary path, it also would result in the excessive energy consumption of the nodes in the primary path. Thus, in EFMRP we design a probability-based traffic allocation scheme: for the k paths $\{l_1, l_2, \ldots, l_k\}$ from source node i to the sink, we can easily get the next-hop collection $Z = \{n_1, n_2, \ldots, n_k\}$ of node i. No matter where the packets come from (*i.e.,* received from the last hop or generated by the node itself), each data transmission is considered as an independent process. For each data packet at node i, the probability of selecting neighboring node n_s as the next hop is

$$P(n_s) = \frac{U_t(n_s)}{\sum_{j=1}^{k} U_t(n_j)}. \tag{17}$$

In (17), each alternative node has been assigned with a path selection probability according to its target potential field value. In this way, on the one hand, the node with higher target potential value can have a larger probability to be selected as the next hop, and on the other hand, the nodes along with the primary path would not be over-exhausted as other paths would share its routing tasks. What is more, the target potential field value is time-varying via neighborhood interaction and global update, making the traffic allocation able to be proactive to the changes of the environment, energy and network topology. For instance, if the impact of node j suffering from external environment tends to be heavier, its target field value $U_t(n_j)$ would be lower, thus making it less likely to be chosen to transmit data packets.

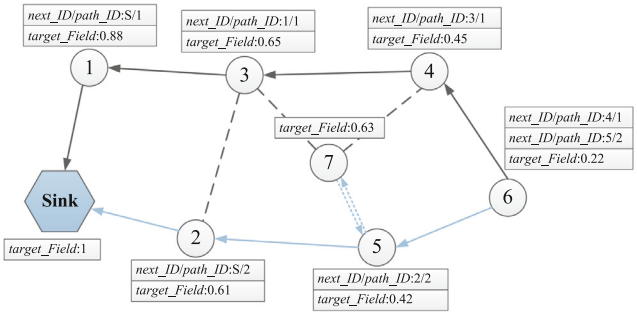

Fig. 5. An example of the retreat mechanism.

5.5. Retreat mechanism

In the multipath discovery, when first receiving a data packet labeled by a new path, the node will broadcast a *QUERY* message to its neighbors to find out which node has not been used yet. There is a special case: all the neighbors have been used and no one is available for next hop. In view of this situation, we design a retreat mechanism to avoid the data packet get into a dead end.

In our retreat mechanism, if sensor node i fails to find proper next hop for a new path through neighbor query, it will send back the data packet to its last-hop node j rather than simply drop it. The last-hop node j will re-check its *ROUTING_TABLE* to find the proper one for the next hop among non-used ones. Since node i has been proven to be a dead end, it will not be selected as the relay node of this path anymore. If node j is still not able to find proper next hop for this path, the data packet will continue to be sent back to the last hop until a new one is discovered to be qualified for next hop. It is worth to note that the *ROUTING_TABLE* will update with the retreat process simultaneously; therefore, the retreat process will only occur in the path discovery phase.

Fig. 5, shows an example of the retreat mechanism in which the node 7 has received a data packet from node 5 and then broadcasts a *QUERY* message to find the forwarder. Since node 3 and node 4 have been used by the primary path, there is no available node to act as a forwarder. According to the implemented retreat mechanism, the data packet will return back to node 5. Node 5 will re-check its *ROUTING_TABLE* and, since node 7 has been proven to be a dead end, the only option is to select node 2 as a forwarder. Then, the *next_ID* that is paired with *source_ID*=6 in the *ROUTING_TABLE* of node 5 will be updated to 2. At the end of this process, the obtained secondary path will be $6 \rightarrow 5 \rightarrow 2 \rightarrow$ sink.

6. Performance evaluation

In this section we describe the simulation environment and discuss the obtained results to validate the proposed EFMRP scheme.

6.1. Simulation setup

We validate the EFMRP using simulation experiments conducted through a self-developed Matlab based simulator. Our simulation environment uses 400 m × 400 m area field in which 200 sensor nodes are randomly. The network topology is shown in Fig. 6. The network is affected by some environmental events (*i.e.,* wildfire and rainstorm). The wildfire event uses the radiation model [44]. In this model, the impact of events decreases with the increase of distance from the event center. In this context, the temperature at the event center will surely destroy the sensor nodes; furthermore, as the distance increases, the temperature will decline and the failure probability of the sensor nodes will decrease accordingly. The rainstorm event uses the uniform distribution model, which is observed from nature. In this model, the event area is block-shaped and the impact brought by this event to the sensor nodes in this area is totally the same. According to the severity of rainstorm

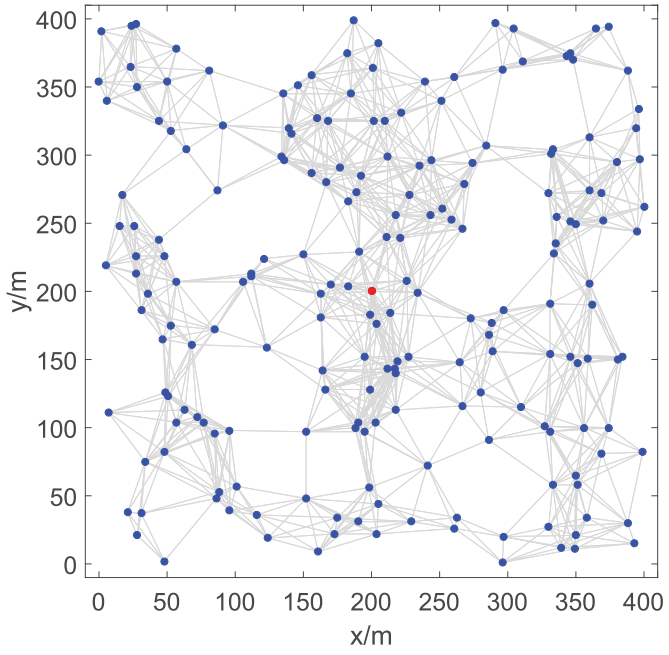

Fig. 6. Network topology.

event, the affected nodes will suffer performance degradation or turn into complete failure.

By referencing to the technical working parameters of MicaZ and TelosB [32], the normal interval for temperature and relative humidity are set to [0,50]°C and [30%,80%] respectively. All nodes are identical with a radio transmission range set to 50 m. The sink node is placed at the center position of the simulation area. Each sensor node senses the area in the vicinity and generates one data packet of 125 bytes. The initial energy of each sensor node is 1 J. The energy consumption model is the first-order radio model proposed in [18]. In this model, the energy consumption of wireless transmission depends on the fixed energy consumption of radio circuitry and the distance between the sender and receiver. To transmit l bits message over a distance d, the energy consumption $E_{Tx}(l, d)$ is

$$E_{Tx}(l,d) = \begin{cases} l \cdot E_{elec} + l \cdot \varepsilon_{fs} \cdot d^2, & \text{if } d \le d_0, \\ l \cdot E_{elec} + l \cdot \varepsilon_{mp} \cdot d^4, & \text{if } d > d_0, \end{cases} \tag{18}$$

where $d_0 = \sqrt{\varepsilon_{fs}/\varepsilon_{mp}}$ is the threshold of the distance and E_{elec} is the electronic energy cost for 1 bit. ε_{fs} is the coefficient of the free space channel model with d^2 power loss and ε_{mp} is the coefficient of the multipath fading channel model with d^4 power loss. The energy cost for receiving l bit message is E_{Rx}

$$E_{Rx}(l) = l \cdot (E_{elec} + E_{da}), \tag{19}$$

where E_{da} is the energy consumption for data aggregation. In the simulations, the log-distance path loss model is used to quantify the link quality [5]. The log-distance path loss model is expressed as

$$PL(d) = PL_0 + 10\eta \log_{10}\frac{d}{d_0} + X_\sigma, \tag{20}$$

where η is the path loss exponent which is 2 for free space and is generally higher for wireless channels. d_0 is the reference distance and PL_0 is the path loss measured at the reference distance d_0. X_σ is a normal random variable with zero mean or a Gaussian random variable with standard deviation σ, reflecting the variation in average received power. We set η=3 and σ=2 in the simulations. We set γ=0.1 and f_{update}=300 s for routing maintenance in the simulations. Table 1 summarizes all the simulation parameters and the simulation results are averaged over 10 independent runs.

6.2. Modeling of environmental impact

To quantify the environmental impact on routing performance, here we categorize the environmental impact into two types: the impact that can cause failure and the impact that can cause performance degradation. In the first case the sensor node stops working due to environmental reasons; for instance, the sensor node is burned by wildfire or short-circled by rainstorm. In the second case the sensor node can still work, but its performance suffers degradation due to environmental reasons; for instance, the sensor node can still transmit data, but its packet loss rate decreases due to electromagnetic interference. We propose two relational models to quantify these two types of impact: *Environmental Failure Model* and *Environmental Degradation Model*.

6.2.1. Environmental failure model

In the environmental failure model, the failure probability of a sensor node is closely related to the external environment and the failure probability function $P_f(i)$ is expressed as

$$P_f(i) = e^{-\lambda U_m(i)}, \tag{21}$$

where λ ($\lambda > 0$) is the tuning coefficient whose purpose is to adjust the impacting level of the environment on node failure behavior. With the

Table 1
Parameter settings.

Parameters	Values
Simulation time	6000 s
Network field	400 m × 400 m
Number of sensors	200
Mobility of sensors	Static
Location of the sink	(200,200)m
Transmission range	50 m
MAC layer	IEEE 802.11
Packet size	125 bytes
Sampling rate	1 packet/2s
Initial energy	1 J
Event types	Wildfire, rainstorm
Event number	From 0 to 4
Event lasting time	From 100 s to 400 s
Event area (wildfire)	Circles with a radius from 5 m and 50 m
Event area (rainstorm)	Block-shape with a coverage from 1000m^2 to 10000m^2
Normal range for temperature	[0,50]°C
Normal range for relative humidity	[30%, 80%]
Extreme range (temperature)	[− 10,100]°C
Extreme range (relative humidity)	[0%, 100%]

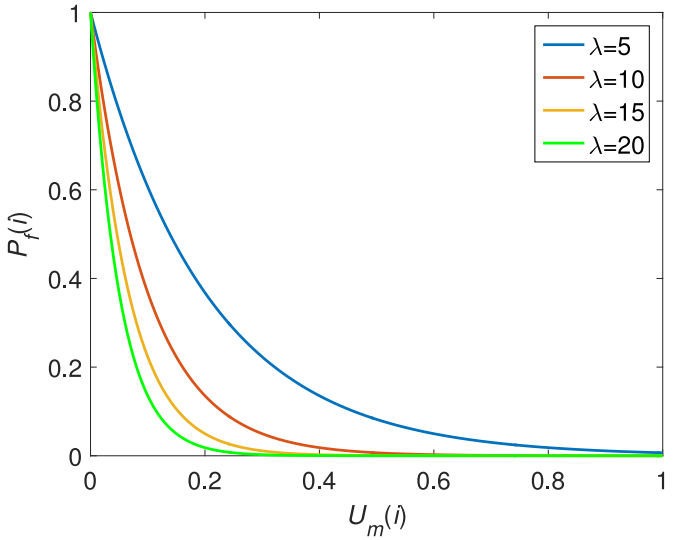

Fig. 7. Failure probability function.

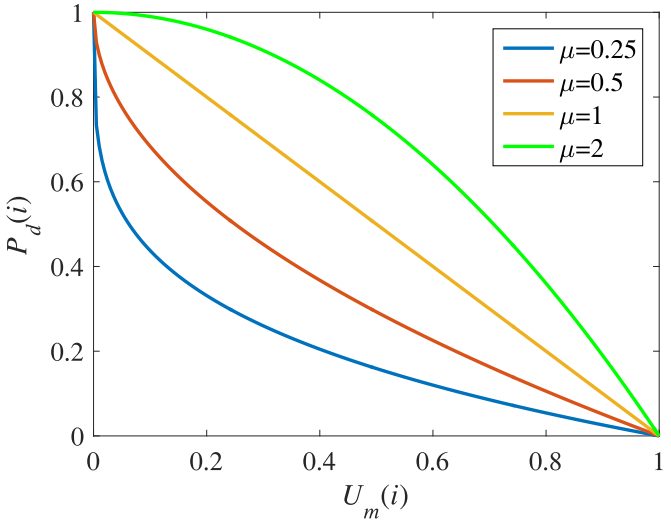

Fig. 8. Degradation probability function.

increase of λ, the relation between node failure and environment tends to be weaker. According to the field design in Section 4, $U_m(i)$ can reflect the impact of multiple environmental factors on routing performance; in particular, $U_m(i)$=1 means that the environmental impact can be ignored. With the decrease of $U_m(i)$, the impact due to the external environment on routing tends to be serious; therefore, in the failure probability function, $U_m(i)$ is selected as the only input. When $U_m(i)$=1, since the environment has little effect on routing, the environment failure probability is very close to zero. With the decrease of $U_m(i)$, the environmental effects tend to be obvious and the environment failure probability tends to decrease in an exponential way.

Since this exponential trend has been demonstrated from the statistics of electric device failure behavior [16], we set λ=10. In our simulations, the failure state of sensor nodes will be updated according to (21) every 100 s and this state is irreversible. The curve of failure probability function is shown in Fig. 7.

6.2.2. Environmental degradation model

In the environmental degradation model, the packet loss probability is related to the external environment. The packet loss probability is defined as the probability of received packets not relaying to the next hop. In this case, the packet loss also tales into account the unstable transmission and running error. The degradation probability function $P_d(i)$ is expressed as:

$$P_d(i) = 1 - U_m(i)^{\mu}, \tag{22}$$

where μ ($\mu > 0$) is the tuning coefficient to take into account the impacting level of the environment on node degradation behavior. When $\mu = 1$, $P_d(i)$ has a linear relational respect to $U_m(i)$. When $\mu > 1$, with the decrease of $U_m(i)$, the packet loss probability tends to incline slower. Conversely, for the case $\mu < 1$, the packet loss probability tends to decline faster with the decrease of $U_m(i)$. Of course, sensor nodes would be influenced more seriously when the temperature drops from 10 °C to 0 °C rather than when temperature decreases from 20 °C to 10 °C; thus, given the degradation law of the sensor nodes, we set μ=0.5. In our simulations, the performance degradation state of sensor nodes updates according to (22) every 100 s and the occurred degradation process is irreversible. The curve of degradation probability function is shown in Fig. 8.

6.3. Performance metric

Several metrics are applied to make a comprehensive performance evaluation.

1. **Network lifetime**: defined as the time when the half amount of sensor nodes turn into failure. Although in some literature, the time until the first sensor node dies is defined as network lifetime, in our opinion, the time when the first node dies cannot indicate that the network lifetime is terminated. If the node at the edge of the network falls into failure, remaining node can still work well and the network performance cannot hardly be affected from the perspective of functionality. At this point, we can reasonably consider that the network lifetime will still continue.
2. **Portion of living nodes (PLN)**: defined as the proportion of nodes that are able to deliver the messages to the sink. It is worth noting that, if a sensor node cannot construct at least one effective path to the sink, we still consider it as a failure node even if it has sufficient energy and its components are still well-functioning. In most cases, being isolated is the major reason responsible for node failures.
3. **Energy Balance Factor (EBF)**: defined as the standard deviation of the residual energy of the sensor nodes. The EBF is calculated as

$$EBF = \sqrt{\frac{1}{n}\sum_{i=1}^{n}\left(E_{res}(i) - E_{ave}\right)^2} \tag{23}$$

where n is the total number of sensor nodes except for the sink, $E_{res}(i)$ is the residual energy of node i and E_{ave} is the average residual energy of all the sensor nodes. EBF is used to measure the energy balance level of the network. A low EBF indicates that the residual energy of the sensor nodes tends to be close to the average residual energy, while a high EBF indicates that the residual energy of the sensor nodes are spread out over a wide range.
4. **Packet delivery ratio (PDR)**: is the ratio of the number of packets successfully received by the sink respect to the total number of packets sent by the sensor nodes.
5. **End-to-end delay**: is the total delay of a data packet from the source node to the sink, including the processing delay, the queueing delay, the transmission delay and the propagation delay. In WSNs, as the data packet size is small and the transmission radius is limited, we can assume that the time spent for each attempt to transmit one packet to the next hop is a constant.

6.4. Path analysis

We select five combinations of EFMRP parameters, listed in Table 2, to evaluate their effects on the multipath discovery. We refer to these parameter combinations as case 1–5 respectively.

Table 2
EFMRP parameters (α, β).

Combination	(α, β)
Case 1	(0,0)
Case 2	(0.2,0)
Case 3	(0,0.2)
Case 4	(0.2,0.2)
Case 5	(0.3,0.3)

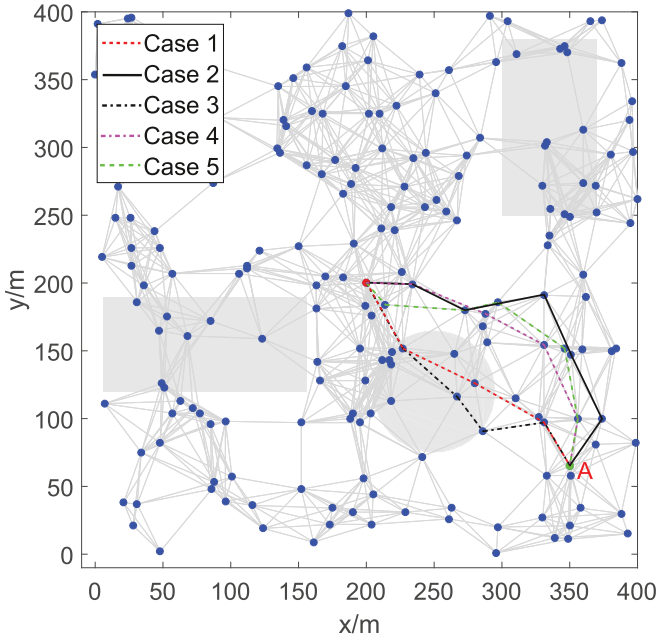

Fig. 9. Primary path with different EFMRP parameter settings (dark zone is the area affected by events).

Fig. 9 shows the primary path from source node A to the sink under various parameters combination. Regarding the case 1, since $\alpha = \beta$=0, the primary path discovery is only determined by depth potential field, making EFMRP to degenerate to the shortest path routing algorithm. From source node A to the sink, the message relay needs 4 hops.

In case 2, routing decisions are jointly made by depth field and environmental field. It can be easily observed that, aiming to bypass the danger zones, it requires more hops (i.e., hop number=6) to reach the sink.

In case 3, besides depth potential field, the routing decision is also affected by residual energy. The constructed path would avoid passing through the poor-energy node.

In case 4, the primary path is created considering depth, energy and environment together. On the one hand, the constructed path avoids danger zones successfully; on the other hand, the energy consumption of the network can be balanced.

In case 5, the weights of environmental field and residual energy field become larger compared with case 4. Although residual energy and environment are fully considered in this case, the directional function of depth field is weakened, thus leading to the increase of path length.

Fig. 10 shows the multiple paths constructed under the same setting (α=0.2, β=0.2). It can be easily observed that, with the increasing number of paths in the network, the hops required by new path would become more. The primary path, only needs 5 hops to reach the sink but in the third path, the required hops increase to 7.

Aiming to ensure node-disjointness, the path that joins the network later cannot overlay with the nodes that participate into the existing paths. Thus, it has to take a longer distance to bypass them. Besides that, the later the path is built, the less option it has for relay selection; hence,

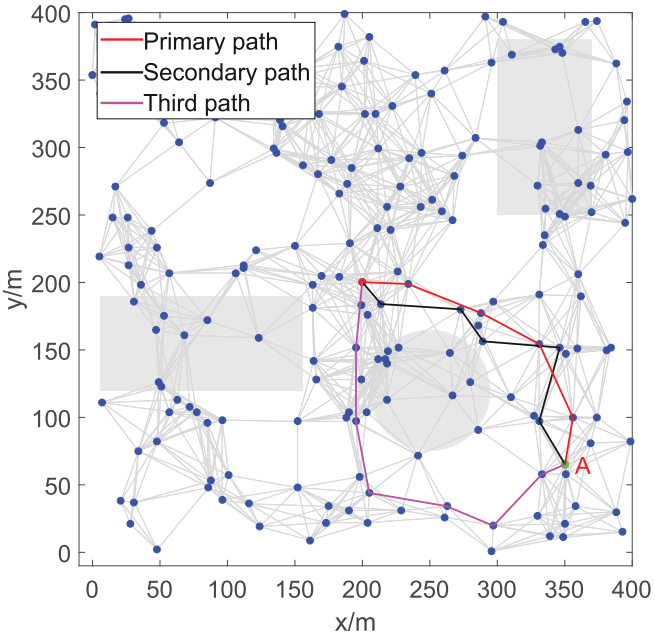

Fig. 10. Multipath with the same parameter settings α=0.2, β=0.2 (dark zone is the area affected by events).

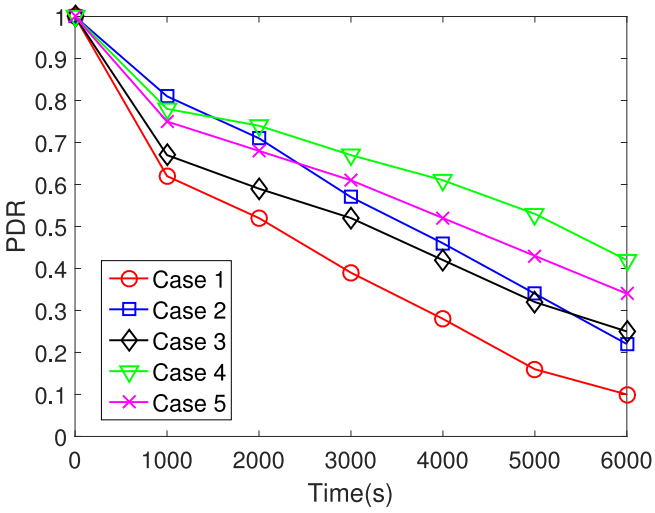

Fig. 11. PDR with different EFMRP parameter settings.

the routing quality of later-jointed path will suffer degradation. In some cases, it has to select poor-energy node or cross through the danger zones because the next-hop nodes that can provide a better service have been already used by other paths.

6.5. *Impact of weighted coefficients*

In this section, we investigated the impact of the weighted coefficients on routing performance. We still used the parameter groups listed in Table 2 but the multipath number is set to 2 (*i.e.,* the primary path and the secondary path).

Fig. 11 shows the PDR (packet delivery ratio) under various settings. At the early phase, case 2 can maintain the highest delivery ratio. Besides depth field, in case 2 the environmental field is the only factor to support routing decisions. Thus, avoiding danger zones to achieve reliable transmission is its first priority but this advantage will be reduced as its energy efficiency is not good enough. Some key nodes will die

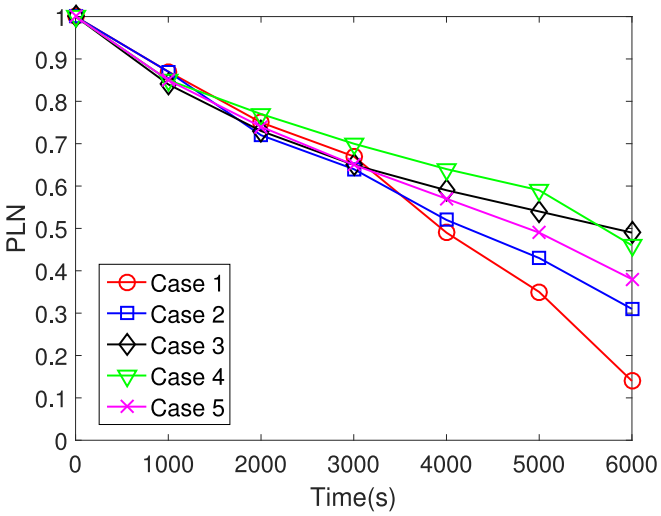

Fig. 12. PLN with different EFMRP parameter settings.

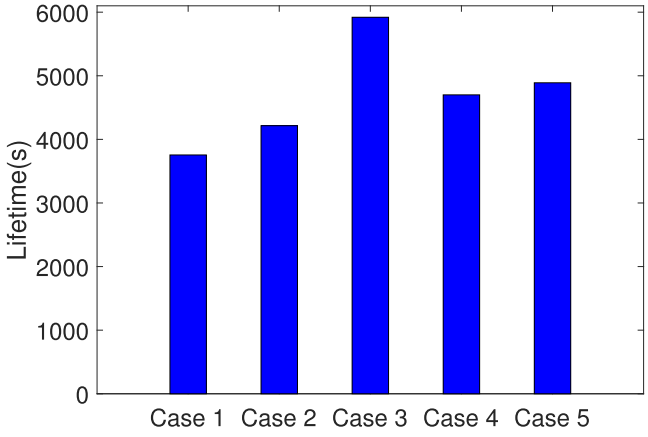

Fig. 13. Lifetime with different EFMRP parameter settings.

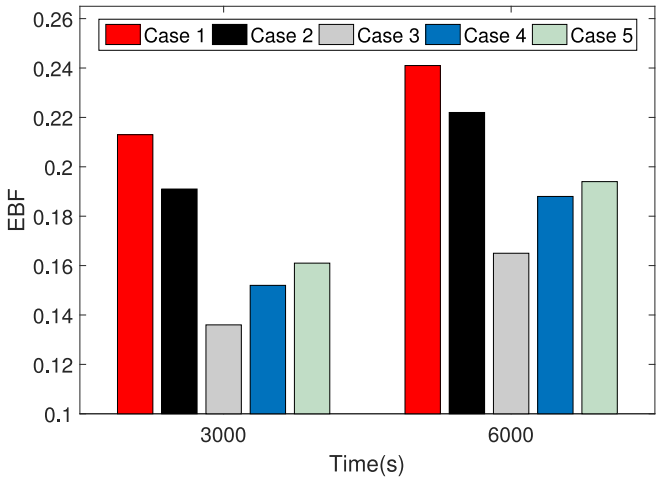

Fig. 14. EBF with different EFMRP parameter settings.

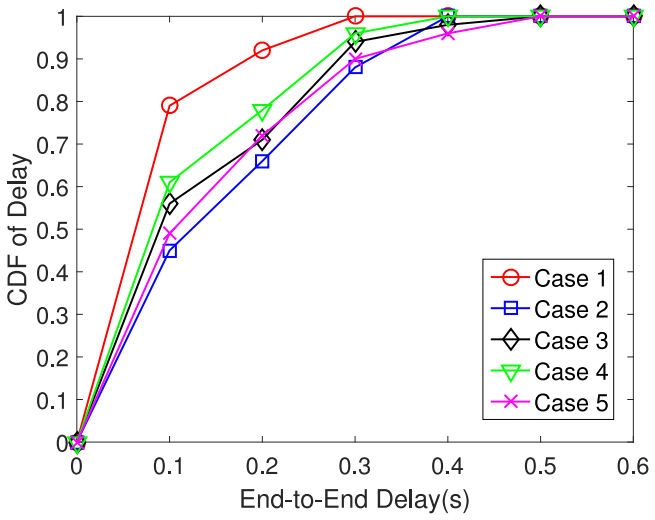

Fig. 15. CDF of delay with different EFMRP parameter settings.

too early due to the energy exhaustion and then it will cause network partition, thus resulting in a dramatic decline in PDR. Regarding the case 4, besides depth field and environmental field, the residual energy field is added to protect low-energy nodes. Although its delivery ratio is slightly lower than case 1 at the early phase, its performance demonstrates a good stability throughout the all simulated period by achieving a greater PDR at the end of the simulation. In case 5, although residual energy and environment are both taken into consideration, its path length would be prolonged as the directional function of depth potential field is over weakened, thus leading to excessive energy consumption.

Figs. 12 and 13 show the PLN (portion of living nodes) and the network lifetime with different EFMRP parameter settings. For case 3, 48% of sensor nodes can still function well at t=6000 s as the energy factor is the only factor to support route discovery besides depth. By contrast, in case 1 only 12% of sensor nodes survive and the lifetime is only two-thirds of the value in case 3. Obviously, ignoring energy factor while making routing decision would make the poor-energy nodes die rapidly, leading to the dramatic decrease of PLN.

In Fig. 14, it is possible to observe that, considering residual energy factors into route discovery (*i.e.,* case 3, case 4 and case 5) turns into much lower EBF values respect to the other two cases, which means that they have better energy-balance level. This further validates the benefits of using residual energy field.

Fig. 15 describes the cumulative distribution function (CDF) of the end-to-end delay. Here, we only count the packets that successfully reach the sink. As expected, the end-to-end delay in case 1 is the shortest as its data packets follow the shortest path to the sink but this advantage is obtained at the expense of low delivery ratio and short lifetime.

The above experimental results demonstrate that different parameter settings can make a significant difference in routing performance. Network lifetime can be beneficial from the larger β. The delivery ratio at the early phase (*i.e.,* all the nodes have sufficient energy) are prone to large α. But for the last phase (*i.e.,* a portion of nodes fail owing to energy exhaustion), a larger β can be more helpful. Regarding the delivery delay, the smaller the $\alpha + \beta$ is, the shorter it will be; thus, to optimize the integrated performance, it is rational to make a tradeoff.

Since the depth field forms the basic routing backbone, the environmental field and the residual energy field act as an assistant to instruct the data packets to follow the appropriate way to the sink. By following this approach, it is reasonable to properly increase the weight of the depth field and let it play a dominant role in the target potential field (*i.e.,* $\alpha + \beta < 0.5$).

This should be one of the practical guidelines in the parameter configuration. The poor performance of case 5 ($\alpha = \beta$=0.3) verifies our analysis. Besides that, the configurations with only effective α or β are hard to provide a satisfactory integrated performance (such as case 1 and case 2). Thus, in parameter configuration, it is necessary to assign reasonable values to α and β. In summary, a recommended parameter configuration

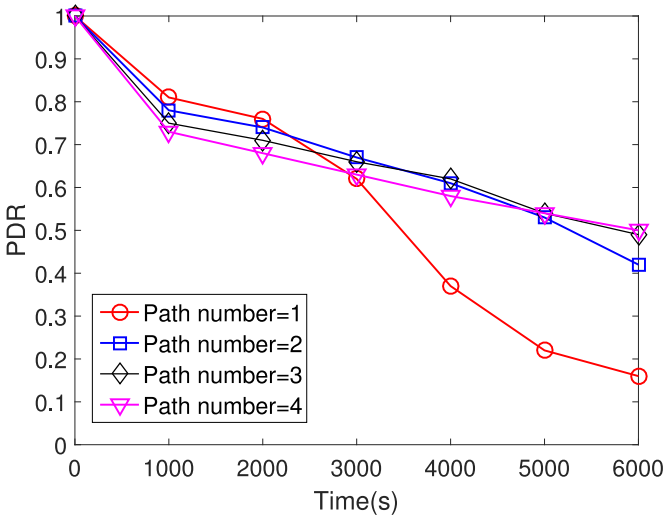

Fig. 16. PDR increasing the numbers of paths.

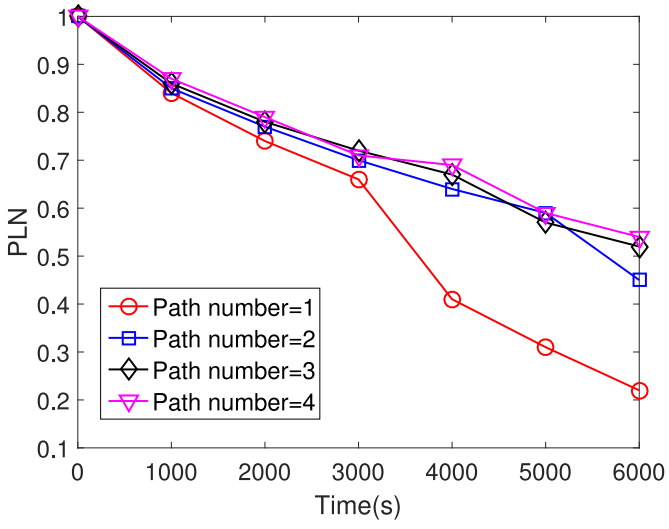

Fig. 17. PLN increasing the numbers of paths.

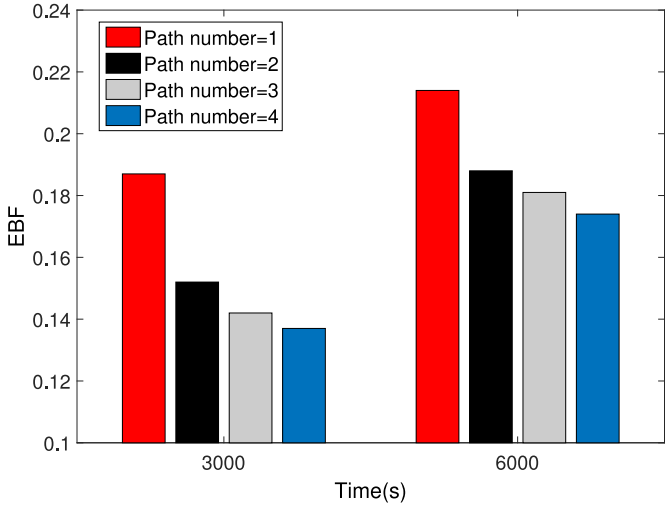

Fig. 18. EBF increasing the numbers of paths.

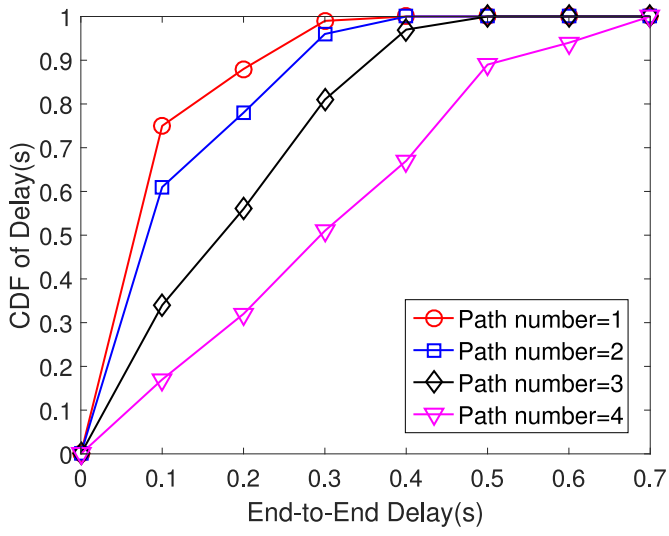

Fig. 19. CDF of delay increasing the numbers of paths.

solution is to choose small α and β at the same time. The favourable integrated performance exhibited by case 4 can confirm this assumption. Moreover, we have repeated many other similar experiments (that we cannot show due to the space limits) by varying network sizes and different parameter values and the obtained results confirm that these basic guidelines toward the parameter settings can be generally adopted.

6.6. Single path vs multipath

In this section, we investigated the benefits of multipath on routing. Given that case 4 has the best routing performance from the comprehensive point of view, here we use the configuration $\alpha = \beta$=0.2 for our experiments.

As is shown in Fig. 16, with the increasing number of paths, the PDR can be improved significantly. When the path number is equal to 1, the delivery ratio is only 0.16 at t=6000 s but when path number increases to 3, the delivery ratio rises to 0.49. This improvement is mostly due to two aspects: 1) the increasing number of paths can reduce the dependence of data transmission on the single path; 2) more paths can alleviate the transmission burden of the single path and make the nodes on these paths live longer.

It is worth noting that the lifting effect of building new paths tends to be less obvious with the increasing number of paths introduced into the routing. From the comparison between path number=3 and path number=4, we can easily discover that the delivery ratio is almost unchanged. This behaviour is to ensure node-disjointness, the later-built path has to avoid the nodes that have been used by existing paths, thus resulting in the degradation of its lifting effect. In other words, compared with the earlier-built path that can choose nodes they prefer, the later-build path can only choose the nodes that are left, making its routing function less satisfactory.

Fig. 17 depicts the PLN increasing the numbers of paths. Similar to the lifting effect of building new paths on PDR, PLN can also be improved as the path number increases. From the comparison between path number=1 and path number=3, we can see that the PLN at time t=6000 s increases from 0.22 to 0.52. When the path number reaches 3, the lifting effect of adding new path meets its upper limit. Obviously, compared with the earlier-built paths that can choose the “safe” nodes, the later-built path has to cross the danger zones as it has no better option, making it easy to be cut off due to environmental reason. Hence, when path number meets its saturation, its “diversion effect” (*i.e.,* share transmission task with other paths) can hardly be further exploited, and the lifting effect of adding new path on energy balance tends to decline with the increasing number of paths introduced into the network. The statistics result shown in Fig. 18 verifies our analysis.

Fig. 19 depicts the CDF of end-to-end delay increasing the numbers of paths. Unlike the lifting effect of building new paths on PDR and network lifetime, the delivery delay tends to be slightly longer with the

Table 3
Parameters settings in routing protocols.

Routing protocols	Parameters	Values
EFMRP	(α, β)	(0.2,0.2)
AODV	T_c	3
SGF	(W_c, W_E, W_R)	(0.5,0.4,0.1)

increasing number of paths. For the later-joint path, aiming to ensure node-disjointness, it cannot overlay with the nodes that participate into the existing paths; thus, it has to take a longer distance to bypass them, resulting in longer delivery delay.

From all the above experiments, we can argue that, within a reasonable scale, adding more paths can improve the network performance with respect to delivery ratio and network lifetime. Despite the fact that adding more paths would cause a slight rise in latency, this cannot affect the lifting effects on network routing. However, an excessive amount of paths cannot bring more benefits; on the contrary, it will result in the rise of routing complexity and energy consumption in the routing discovery phase. Through experiments under various network settings, we find that it is better to set the path number as the half of average neighbor number (*i.e.,* average network degree). In this configuration, even for the last-joined path, it still can choose the qualified node as the relay from the remaining half neighbors. Clearly, according to our guideline, as the node density becomes higher, the required path number will also increase. In the current experiment, the average network degree is 6.2 and its optimum path number should be 3 according to our guideline. The favorable performance of path number=3 can further verify our guideline.

6.7. Comparison

In this section, we compare EFMRP with two commonly used node-disjoint multipath protocols: SGF [20] and AODV [31]. To be fair, the multipath numbers in all three routing protocols are set to 3. The routing parameters in SGF and AODV are set according to the recommended configurations in their literature which are shown in Table 3.

As shown in Fig. 20, we can easily observe that EFMRP performs better among the three routing protocols, SGF comes second and the last is AODV. Since both EFMRP and SGF take into consideration the energy factor to make routing decisions, they can outperform AODV in PDR due to their energy-balance feature. Specifically, using AODV, the "hot spot" issue will drain the energy of key nodes very fast and then make the

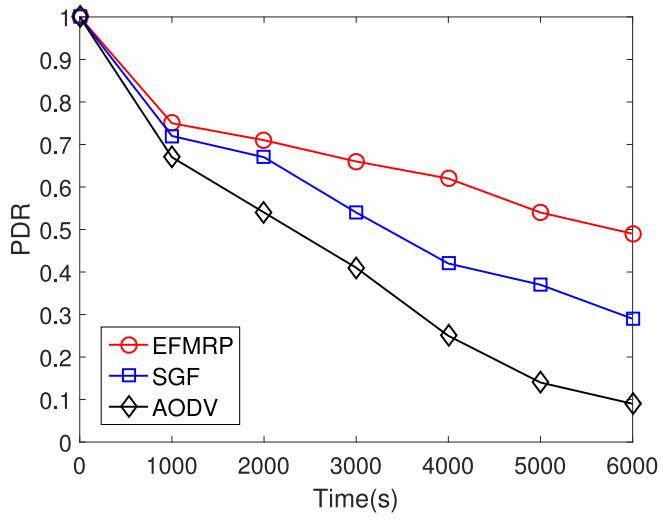

Fig. 20. PDR with different routing protocols.

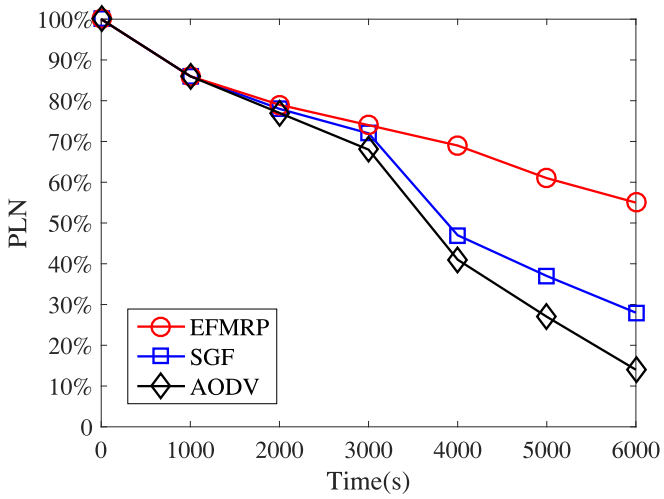

Fig. 21. PLN with different routing protocols.

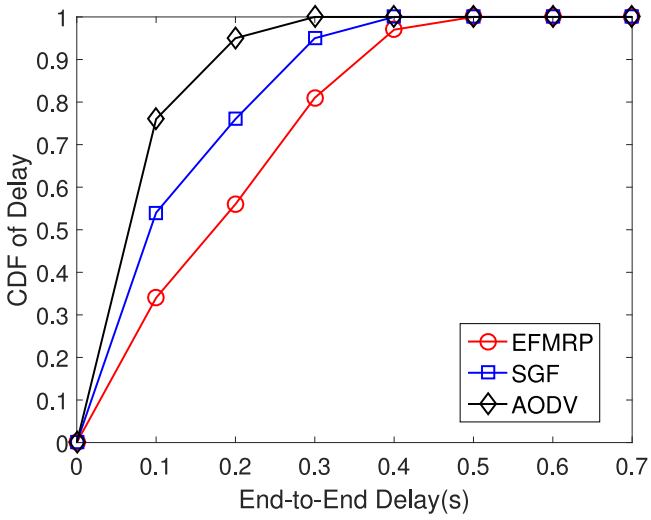

Fig. 22. CDF of delay with different routing protocols.

network to collapse. In particular, since EFMRP is environment-aware and can avoid danger zones, the constructed paths are much less likely to be cut off, due to environmental reasons, than those computed by SGF; this explains the reason why EFMRP is superior to SGF in terms of PDR.

As shown in Fig. 21, the performance rank in terms of PLN is the same as that in PDR. According to our definition of network lifetime, AODV can only last for t=3600 s. Obviously, the "hot spot" issue should be responsible for that. SGF and EFMRP can live longer due to their energy-balance feature. Since the SGF does not consider environmental impact, its paths are prone to be interrupted. As more and more paths are cut off due to the environmental reasons, its concentration level of data transmission will be higher. For instance, considering the path number=3 from the source node to the sink, if two paths are interrupted, the entire transmission task would be concentrated into the last path; thus, the energy-balance feature will be severely weakened. On the contrary, EFMRP can make better use of its energy-balance feature due to high path survival rate. In other words, environment-awareness can help the selected paths live longer and make them share the transmission tasks as long as possible. This motivates why EFMRP can perform better than SGF in PLN and PDR.

Finally, Fig. 22, shows that the delivery delay of AODV is the shortest among three routing protocols. Since the basic idea of AODV is to dis-

cover the shortest path towards the sink, its latency can be minimized. However this advantage in delivery delay cannot compensate the poor performance in PLN and PDR. In most of the cases, EFMRP needs to take a longer path in order to avoid danger zones, thus it is evident that it will spend more time to reach the sink than SGF.

In general, through comparison experiments, we can easily get that EFMRP can have better performance than other two routing protocols in PLN and PDR. To some extent, these advantages need to sacrifice the latency; however, the main priority of WSNs is to send data to the sink successfully, therefore this sacrifice is worthwhile.

7. Conclusions

As most of the WSNs are deployed in unattended scenarios and are also constrained by limited energy and low cost, the network performance would be easily affected by energy factor and environmental factors. Most of the current research related to WSN routing has only considered energy factor without taking into account the environmental impact on routing performance. Neglecting environmental impact would make the constructed routing paths vulnerable to the external environmental changes.

To tackle this issue, we proposed an environment-fusion routing multipath routing protocol EFMRP. The main contributions include: 1) the proposal of a modeling method of potential field to instruct data packets to reach the sink. The final field is a hybrid field creating by environmental field, depth field and energy field, which means that the routing decision is made according to the depth, energy and environment; 2) the design of maintenance mechanism, traffic allocation mechanism and retreat mechanism to ensure EFMRP working efficiently.

The presented simulation results show that the proposed EFMRP solution makes significant improvements in delivery ratio, network lifetime and energy balance compared with the commonly used protocols. We also found that although adding more paths can improve the network performance with respect to delivery ratio and network lifetime, an excessive amount of paths cannot bring more benefits. As further insight, we can argue that making routing environment-aware can bring benefits from two sides: 1) when the network encounters the emergency (*e.g.,* wildfire), the routing can make real-time decisions to select paths far away from the danger zones in order to guarantee sustainable data delivery; 2) from the long-term perspective, since the paths are more invulnerable to the external environment, they can share the transmission tasks as long as possible, thus improving the energy-balance level and prolonging the network lifetime.

In this paper, we only give a theoretical analysis of effects of routing parameters (α and β) on message forwarding and provide some guidelines about settings of α and β. In the next step of our work, we plan to design a weight decision method to get the perfect value of α and β. By using this method, the users can get the recommended settings according to their performance requirements and the practical network situations. In addition, in this work, we mainly focus on the single-sink WSNs. Due to the advantages in load balancing and energy conservation, multi-sink WSNs have been received more and more attention. Therefore, upgrading EFMRP to make it suitable for multi-sink WSNs will also be the focus of our future work.

Acknowledgment

This work is supported in part by the National Natural Science Foundation of China (NSFC) under Grant no. 61571336 and 61603280.

Declaration of Competing Interest

None.

References

[1] A. Abrardo, M. Martalò, G. Ferrari, Information fusion for efficient target detection in large-scale surveillance wireless sensor networks, Inf. Fusion 38 (2017) 55–64.
[2] F. Al-Turjman, M. Z. Hasan, Optimized multi-constrained quality-of-service multi-path routing approach for multimedia sensor networks, IEEE Sensors Journal PP (99) 1–1.
[3] E.V. Aleksandrova, V.A. Bashkin, Hydrodynamic model of adaptive routing for large-scale unstable sensor networks, in: IEEE International Conference on Control and Communications, 2016, pp. 1–6.
[4] S.H. Chang, M. Merabti, H.M. Mokhtar, Coordinate magnetic routing for mobile sinks wireless sensor networks, in: IEEE International Conference on Advanced Information Networking and Applications, 2007, pp. 846–851.
[5] Y. Chen, A. Terzis, On the implications of the log-normal path loss model: an efficient method to deploy and move sensor motes, in: ACM Conference on Embedded Networked Sensor Systems, 2011, pp. 26–39.
[6] L. Cheng, J. Niu, J. Cao, S.K. Das, Y. Gu, Qos aware geographic opportunistic routing in wireless sensor networks, IEEE Trans. Parallel Distrib. 25 (7) (2014) 1864–1875.
[7] B. Cody-Kenny, D. Guerin, D. Ennis, R.S. Carbajo, M. Huggard, C.M. Goldrick, Performance evaluation of the 6lowpan protocol on Micaz and Telosb motes, Acm Workshop on Performance Monitoring & Measurement of Heterogeneous Wireless & Wired Networks, 2009.
[8] B. Deb, S. Bhatnagar, B. Nath, Reinform: reliable information forwarding using multiple paths in sensor networks, in: IEEE International Conference on Local Computer Networks, 2003. LCN '03. Proceedings, 2003, pp. 406–415.
[9] S. Dong, Z. Gao, S. Pirbhulal, G.-B. Bian, H. Zhang, W. Wu, S. Li, Iot-based 3d convolution for video salient object detection, Neural Comput. Appl. (2019) 1–12.
[10] Y. Duan, X. Fu, W. Li, Y. Zhang, G. Fortino, Evolution of scale-free wireless sensor networks with feature of small-world networks, Complexity 2017 (3) (2017) 1–15.
[11] Y. Duan, Y. Luo, W. Li, P. Pace, G. Aloi, G. Fortino, A collaborative task-oriented scheduling driven routing approach for industrial iot based on mobile devices, Ad Hoc Netw. 81 (2018) 86–99.
[12] G. Fortino, W. Russo, C. Savaglio, W. Shen, M. Zhou, Agent-oriented cooperative smart objects: from iot system design to implementation, IEEE Trans. Systems Man Cybern. (99) (2017) 1–18.
[13] X. Fu, G. Fortino, W. Li, P. Pace, Y. Yang, Wsns-assisted opportunistic network for low-latency message forwarding in sparse settings, Future Gener. Comput. Syst. 91 (2019) 223–237.
[14] X. Fu, H. Yao, Y. Yang, Exploring the invulnerability of wireless sensor networks against cascading failures, Inf. Sci. 491 (2019) 289–305.
[15] X. Fu, H. Yao, Y. Yang, Modeling and analyzing cascading dynamics of the clustered wireless sensor network, Reliab. Eng. Syst. Saf. 186 (2019) 1–10.
[16] G. Georgakos, U. Schlichtmann, R. Schneider, S. Chakraborty, Reliability challenges for electric vehicles: from devices to architecture and systems software, in: Design Automation Conference, 2013.
[17] R. Gravina, P. Alinia, H. Ghasemzadeh, G. Fortino, Multi-sensor fusion in body sensor networks: state-of-the-art and research challenges, Inf. Fusion 35 (2016) 68–80.
[18] W.R. Heinzelman, A. Chandrakasan, H. Balakrishnan, Energy-efficient communication protocol for wireless sensor networks, in: IEEE International Conference on System Sciences, 2000, p. 8020.
[19] S.P. Hemnani, R. Syed, S. Saleem, M. Mustaqim, N. Kamlesh, Ebm: a cross-layer approach for wireless body area networks, J. Emerg. Trends Comput.Inf. Sci. 7 (2) (2016) 69–76.
[20] P. Huang, H. Chen, G. Xing, Y. Tan, Sgf: a state-free gradient-based forwarding protocol for wireless sensor networks, ACM Trans. Sens. Netw. 5 (2) (2009) 14.
[21] G. Iacca, A. Tejada, A. Liotta, Spatial anomaly detection in sensor networks using neighborhood information, Inf. Fusion 33 (C) (2017) 41–56.
[22] S. Jannu, P.K. Jana, A grid based clustering and routing algorithm for solving hot spot problem in wireless sensor networks, Wirel. Netw. 22 (6) (2016) 1901–1916.
[23] Khatib, Real-time obstacle avoidance for manipulators and mobile robots, Int. J. Robot. Res. 5 (5) (1986) 500–505.
[24] D. Kominami, M. Sugano, M. Murata, T. Hatauchi, Controlled and self-organized routing for large-scale wireless sensor networks, ACM Trans. Sens. Netw. 10 (1) (2013) 13.
[25] A. Kumar, S. Varma, Geographic node-disjoint path routing for wireless sensor networks, IEEE Sens. J. 10 (6) (2010) 1138–1139.
[26] T.W. Kuo, M.J. Tsai, On the construction of data aggregation tree with minimum energy cost in wireless sensor networks: Np-completeness and approximation algorithms, in: IEEE International Conference on Computer Communications (INFOCOM), 2014, pp. 2591–2595.
[27] S. Li, R.K. Neelisetti, C. Liu, A. Lim, Efficient multi-path protocol for wireless sensor networks, Int. J. Wirel. Mob.Netw. 2 (1) (2010) 110–130.
[28] Y. Liu, M. Dong, K. Ota, A. Liu, Activetrust: secure and trustable routing in wireless sensor networks, IEEE Trans. Inf. Forensic Secur. 11 (9) (2017) 2013–2027.
[29] W. Lou, An efficient N-to-1 multipath routing protocol in wireless sensor networks, in: IEEE International Conference on Mobile Adhoc and Sensor Systems, 2005, pp. 664–672.
[30] W. Lou, Y. Kwon, H-SPREAD: a hybrid multipath scheme for secure and reliable data collection in wireless sensor networks, IEEE Trans. Veh. Technol. 55 (4) (2006) 1320–1330.
[31] M. Marina, S. Das, On-demand multi path distance vector routing in ad hoc networks, in: IEEE International Conference on Network Protocols, 2001, pp. 14–23.
[32] C. Pham, Communication performances of IEEE 802.15.4 wireless sensor motes for data-intensive applications: a comparison of waspmote, arduino mega, telosb, micaz and imote2 for image surveillance, J. Netw. Comput. Appl. 46 (2014) 48–59.

[33] S. Pirbhulal, H. Zhang, M. E Alahi, H. Ghayvat, S. Mukhopadhyay, Y.-T. Zhang, W. Wu, A novel secure iot-based smart home automation system using a wireless sensor network, Sensors 17 (1) (2017) 69.
[34] A.A.M. Rahat, R.M. Everson, J.E. Fieldsend, Evolutionary multi-path routing for network lifetime and robustness in wireless sensor networks, Ad Hoc Netw. 52 (2016) 130–145.
[35] F. Ren, J. Zhang, T. He, C. Lin, S.K.D. Ren, Ebrp: energy-balanced routing protocol for data gathering in wireless sensor networks, IEEE Trans. Parallel Distrib. 22 (12) (2011) 2108–2125.
[36] T. Shu, M. Krunz, S. Liu, Secure data collection in wireless sensor networks using randomized dispersive routes, IEEE Trans. Mob.Comput. 9 (7) (2010) 941–954.
[37] A.H. Sodhro, S. Pirbhulal, A.K. Sangaiah, Convergence of iot and product lifecycle management in medical health care, Future Gener. Comput. Syst. 86 (2018) 380–391.
[38] A.H. Sodhro, A.K. Sangaiah, S. Pirphulal, A. Sekhari, Y. Ouzrout, Green media-aware medical iot system, Multimed. Tools Appl. 78 (3) (2019) 3045–3064.
[39] W. Su, M. Alzaghal, Channel propagation characteristics of wireless micaz sensor nodes, Ad Hoc Netw. 7 (6) (2009) 1183–1193.
[40] X. Sun, H. Chen, X. Wu, X. Yin, W. Song, Opportunistic communications based on distributed width-controllable braided multipath routing in wireless sensor networks, Ad Hoc Netw. 36 (P1) (2016) 349–367.
[41] Q. Tang, N. Tummala, S.K.S. Gupta, L. Schwiebert, Tara: thermal-aware routing algorithm for implanted sensor networks, in: IEEE International Conference on Distributed Computing in Sensor Systems, 2005, pp. 206–217.
[42] J. Wang, Y. Zhang, J. Wang, Y. Ma, M. Chen, Pwdgr: pair-wise directional geographical routing based on wireless sensor network, IEEE Internet Things J. 2 (1) (2015) 14–22.
[43] Z. Wang, E. Bulut, B.K. Szymanski, Energy efficient collision aware multipath routing for wireless sensor networks, in: IEEE International Conference on Communications, 2009, pp. 91–95.
[44] D.R. Weise, G.S. Biging, A qualitative comparison of fire spread models incorporating wind and slope effects., Forest Sci. 43 (2) (1997) 170–180. (11)
[45] S. Yi, P. Naldurg, R. Kravets, Security-aware ad hoc routing for wireless networks, in: ACM International Symposium on Mobile Ad Hoc Networking & Computing, 2001, pp. 299–302.
[46] J. Zhao, J.C. Zeng, An electrostatic field-based coverage-enhancing algorithm for wireless multimedia sensor networks, in: IEEE International Conference on Wireless Communications, *Networking* and Mobile Computing, 2009, pp. 1–5.